Available online at www.sciencedirect.com

SciVerse ScienceDirect

Advances in Space Research 51 (2013) 10–20

ADVANCES IN SPACE RESEARCH (a COSPAR publication)

www.elsevier.com/locate/asr

Multi-Sphere Method for modeling spacecraft electrostatic forces and torques

Daan Stevenson *, Hanspeter Schaub

Department of Aerospace Engineering Sciences, University of Colorado, 431 UCB, Colorado Center for Astrodynamics Research, Boulder, CO 80309-0431, United States

Received 16 March 2012; received in revised form 28 August 2012; accepted 30 August 2012
Available online 7 September 2012

Abstract

The use of electrostatic (Coulomb) actuation for formation flying is attractive because non-renewable fuel reserves are not depleted and plume impingement issues are avoided. Prior analytical electrostatic force models used for Coulomb formations assume spherical spacecraft shapes, which include mutual capacitance and induced effects. However, this framework does not capture any orientation-dependent forces or torques on generic spacecraft geometries encountered during very close operations and docking scenarios. The Multi-Sphere Method (MSM) uses a collection of finite spheres to represent a complex shape and analytically approximate the Coulomb interaction with other charged bodies. Finite element analysis software is used as a truth model to determine the optimal sphere locations and radii. The model is robust to varying system parameters such as prescribed voltages and external shape size. Using the MSM, faster-than-realtime electrostatic simulation of six degree of freedom relative spacecraft motion is feasible, which is crucial for the development of robust relative position and orientation control algorithms in local space situational awareness applications. To demonstrate this ability, the rotation of a cylindrical craft in deep space is simulated, while charge control from a neighboring spacecraft is used to de-spin the object. Using a 1 m diameter craft separated by 10 m from a 3 by 1 m cylindrical craft in deep space, a 2 deg/s initial rotation rate can be removed from the cylinder within 3 days, using electric potentials up to 30 kV.

Keywords: Coulomb formations; Electrostatic force model

1. Introduction

As the complexity of spaceflight missions increases, formation flying scenarios can provide beneficial contributions to the science objectives and assurance of mission success. Conventionally, relative position maneuvers are performed using external thrusters that convert fuel into exhaust plumes directed into space. One obvious drawback of this type of propulsion is the costly expenditure of non-renewable fuel reserves, especially in high accuracy relative orbits where frequent position corrections are necessary. Moreover, there is potential for exhaust plume impingement, where thruster exhaust from one craft causes interference with its neighbor's sensors. An attractive alternative is the emerging Coulomb charge control technology. The electrostatic potential of multiple spacecraft can be controlled within microseconds using electron gun or cathode devices, and the resulting Coulomb forces can be used to affect relative spacecraft positions within a formation (King et al., 2002, 2003; Schaub et al., 2004).

Applications of Coulomb charge control include Separated Spacecraft Interferometry (SSI), to achieve large field-of-view planetary imagery with unprecedented resolution, spacecraft docking by electrostatic tractor concepts, and small-body relative orbits with cameras or other robotic devices to inspect external spacecraft integrity. Electrostatic tugs may also be used to deorbit space debris, for if a spacecraft can impart relative potentials on itself

* Corresponding author. Tel.: +1 3034926734.
E-mail addresses: daan.stevenson@colorado.edu (D. Stevenson), hanspeter.schaub@colorado.edu (H. Schaub).

0273-1177/$36.00 © 2012 COSPAR. Published by Elsevier Ltd. All rights reserved.
http://dx.doi.org/10.1016/j.asr.2012.08.014

and an inactive craft using a focused charged beam, touchless re-orbiting maneuvers may be achieved (Schaub and Moorer, 2010; Schaub and Jasper, 2011; Hogan and Schaub, 2011). One limitation of this technology is the effect of plasma in the near-Earth space environment, which causes considerable Debye shielding of the electrostatic fields at LEO. Spacecraft formations at GEO, however, can exert significant electrostatic forces at separation distances of tens of meters, because nominal Debye lengths there are roughly 180–200 m (Tribble, 2003; Denton et al., 2005).

Several studies analyze the relative motion dynamics of a 2 to N craft Coulomb formation (Berryman and Schaub, 2007; Vasavada and Schaub, 2008; Hogan and Schaub, 2012). Complex charge control strategies have been developed that compensate for the nonlinear nature of the electrostatic forces and coupling with differential gravity (Parker et al., 2004; Schaub et al., 2006; Schaub, 2005; Natarajan and Schaub, 2006). In such work spacecraft electrostatics are generally modeled by point charges, while in actuality a voltage is prescribed and enforced by the charge control methods. The electrostatic charge density on the conducting surface is then a result of the spacecraft geometry and external potential fields. For experimental verification of relative motion by Coulomb charge control, physical conducting spheres are used to represent spacecraft bodies (Seubert and Schaub, 2009a,b). To model these interactions, both the mutual capacitance between conducting spheres (Smythe, 1968; Sliško and Brito-Orta, 1998) and induced charging effects (Soules, 1990) are considered to determine the voltage to charge relationship.

Realistically, spacecraft components such as solar panels result in geometries that are far from spherical. When charged bodies interact with separation distances on the order of the spacecraft dimensions, especially in the small body circumnavigation scenario, a model that assumes spherical conductors can result in considerable errors in the electrostatic force prediction. Charge prediction errors of 10% (which can easily result from geometry approximations) have been shown to cause up to 15% errors in relative position control (Hogan and Schaub, 2011). Jasper and Schaub, 2011 proposes to overcome these inaccuracies with an Effective Sphere Method (ESM). Here a finite sphere is used to model the spacecraft body with an effective radius that best captures the electrostatic response over a range of separation distances to an external object. If expanded to 1st order, the effective radius can change depending on spacecraft orientation to capture non-spherical effects. While this approach allows for a very simple analytical force prediction, it compromises accuracy of the Coulomb force at small spacecraft separation distances. Perhaps more importantly, the ESM lacks the ability to resolve electrostatic torques and non line-of-sight forces that result from non-symmetric spacecraft bodies. This is crucial when relative attitudes and small separation distances on the order of the spacecraft dimensions are a consideration in the formation flight mission scenario. When the separation distance exceeds 20 times the spacecraft dimensions, the ESM is a sufficiently accurate and has a lower computational cost than the new method.

This paper introduces a new approach called the Multi-Sphere Method (MSM). Essentially, the electrostatics of a spacecraft with a conducting outer surface held at a fixed voltage is approximated by filling the geometry with multiple finite spheres held at a constant voltage. Because the charge on each sphere is allowed to vary as determined by the mutual capacitance matrix, a similar freedom in the charge distribution throughout the spacecraft is seen as in a generic conducting geometry. As such, the model is robust for various orientations and separation distances, while the accuracy of the model depends on how many spheres are used. The challenge with the MSM is in choosing the size and location of a prescribed number of spheres for a given spacecraft shape. The truth model used for this purpose is Ansoft's Finite Element Method (FEM) software suite Maxwell 3D©. FEM creates a highly accurate but computationally expensive solution of the electrostatic potential fields by finding linearized solutions for Poisson's equation on each finite element in the entire 3D space, with boundary conditions created from the spacecraft geometries and potentials. On their own, the FEM solvers are not capable of faster-than-realtime charged relative motion simulations, and therefore do not provide analytical insight into the dynamics and control of such scenarios.

The MSM methodology, by comparison, resolves forces and torques on the body by iterating Coulomb's law over the charge found on each sphere in the model due to their mutual and self capacitance. This paper examines how to determine best-fit MSM parameters for any specific shape, and discusses the accuracies and limitations of this approach. Further, numerical simulations illustrate how this model can be applied to study the use of electrostatic torque to change the spin of a passive body.

2. Multi-Sphere Method theory

The Multi-Sphere Method (MSM) is a means to approximate the electrostatic interactions between conducting objects with generic geometries. A rigid spacecraft or space debris object is modeled by a collection of spheres with fixed sizes and relative positions, as shown in Fig. 1. Generally, an external sphere is used to resolve the forces and torques on the body so that an optimal solution of the model parameters can be determined. In this section, we assume that the optimal relative positions and sizes of the n spheres in the model has already been determined, for which the process is discussed in the following section. Once these parameters are known, the electrostatic dynamics of a modeled spacecraft can be predicted by replacing its geometry with the finite spheres, which are constrained to match the translation and rotation of the actual body. At this point the external sphere can also be replaced by another generic geometry represented by a MSM. Each

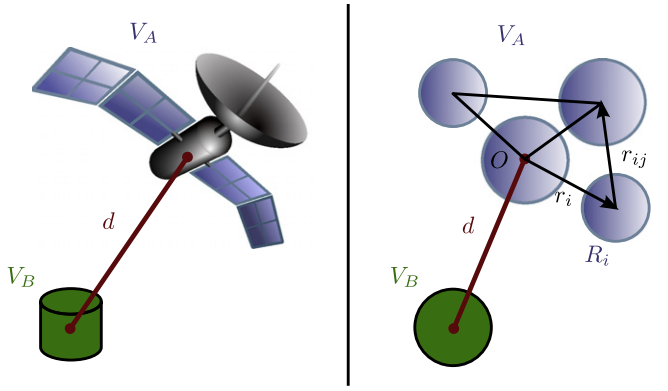

Fig. 1. Conceptual depiction of Multi-Sphere Method.

object requires a specified origin, such as O for the spacecraft in Fig. 1. The system origin can be chosen anywhere.

While the absolute electrostatic voltage is assumed to be prescribed on a spacecraft, the Coulomb force between the spheres is dependent on the charge that each holds. The voltage V_i on a given sphere is a result of both the charge on that sphere and the charges on its neighboring spheres. The relation is given in Eq. (1) (Smythe, 1968; Sliško and Brito-Orta, 1998), where R_i represents the radius of the sphere in question and $\boldsymbol{r}_{i,j} = \boldsymbol{r}_j - \boldsymbol{r}_j$ is the center-to-center distance to each neighbor. The constant $k_c = 8.99\times 10^9\ \mathrm{Nm^2/C^2}$ is Coulomb's constant, and q_i stands for the charge on a given sphere.

$$V_i = k_c\frac{q_i}{R_i} + \sum_{j=1,j\neq i}^{m} k_c\frac{q_j}{r_{i,j}} \tag{1}$$

Note that this relationship is most valid when $r_{ij} \gg R_i$. When the spheres are large and closely spaced, there are limitations in the model, which are discussed throughout the paper in the context of its inability to capture induced charge effects. When more spheres are introduced and their size decreases relative to the system, as is the topic of future research, results become more accurate.

The linear relations for each of the $m = n + 1$ spheres in the system (n spheres in the MSM plus the external sphere) can be combined in the matrix form of Eq. (2), where $\boldsymbol{V} = [V_A, V_A, \ldots, V_A, V_B]^T$ and $\boldsymbol{q} = [q_1, q_2, \ldots, q_n, q_B]^T$ represent matrix collections of the voltages and charges in the entire system.

$$\boldsymbol{V} = k_c[C_M]^{-1}\boldsymbol{q} \tag{2}$$

Notice that V_A is the prescribed voltage on all spheres in the model while the external sphere is held at V_B. The effects of varying the voltage on different spheres within the model have not been analyzed, but keeping the voltage constant is logical since the modeled conducting spacecraft would be held at uniform voltage. This approach also reduces the number of modeled parameters.

The inverse of the position-dependent capacitance matrix in Eq. (2), $[C_M]^{-1}$, can be expanded as follows, according to the nomenclature adopted in Fig. 1, with $\boldsymbol{r}_{i,B} = \boldsymbol{d} - \boldsymbol{r}_i$:

$$[C_M]^{-1} = \begin{bmatrix} 1/R_1 & 1/r_{1,2} & \cdots & 1/r_{1,n} & 1/r_{1,B} \\ 1/r_{2,1} & 1/R_2 & \ddots & \vdots & \vdots \\ \vdots & \ddots & \ddots & \vdots & \vdots \\ 1/r_{n,1} & \cdots & \cdots & 1/R_n & 1/r_{n,B} \\ 1/r_{B,1} & \cdots & \cdots & 1/r_{B,n} & 1/R_B \end{bmatrix} \tag{3}$$

The next step is to solve for the array of charges $\boldsymbol{q}$ from Eq. (2) by inverting this $n+1$ size symmetric matrix, a computation that becomes increasingly intensive when more spheres are used in the model. Coulomb's law can then be implemented to calculate the linear force between each charged sphere. Each body is assumed rigid, such that location of the spheres within the modeled body are held fixed with respect to each other. Their equal and opposite force contributions cancel within the body. The total force $\boldsymbol{F}$ and torque $\boldsymbol{L}$ about the origin O on body A due to external sphere B that results is given by the following summations.

$$\boldsymbol{F} = k_c q_B \sum_{i=1}^{n} \frac{q_i}{r_{i,B^3}}\boldsymbol{r}_{i,B} \tag{4}$$

$$\boldsymbol{L}_O = k_c q_B \sum_{i=1}^{n} \frac{q_i}{r_{i,B^3}}\boldsymbol{r}_i \times \boldsymbol{r}_{i,B} \tag{5}$$

Note that while any origin can be chosen for body A, the force and torque in Eqs. (4) and (5) are now defined from this reference origin. To determine the electrostatic kinetics between two bodies modeled using the Multi-Sphere Method, the external sphere B would be replaced with a collection of spheres using the same formulation as for body A. The force and torque relations will then contain double summations.

While the MSM does not provide an analytic solution for the Coulomb interactions for any number of spheres, due to the $n + 1$ dimensional matrix inversion, this computation is much faster than current FEM solvers. As such, relative spacecraft motion due to inter-formation actuation can be predicted in real time and incorporated in control algorithms. One is left with the task of choosing optimal parameters of the sphere and verifying the fidelity of the model, which is the focus of the remainder of this paper.

2.1. FEM truth data

A reliable electrostatics solver is necessary to determine an optimal parameter set for the MSM and verify its accuracy. While the accuracy of the experimental verification of relative Coulomb motion is gaining ground (Seubert and Schaub, 2010), the disturbance errors are still an order of magnitude larger than the small 3D shape effects for which this model hopes to compensate. Analytical solutions to Poisson's equation (by multipole expansion) in a system with charged conductors are only available for the simplest

isolated geometries (Soules, 1990). When the boundary conditions become more complex, FEM solvers can create linearized solutions of Poisson's equations at each element, from which charge distributions and forces can be derived. Out of the wide range of commercially available electrostatic modeling software, Ansoft Maxwell 3D (http://www.ansoft.com/products/em/maxwell) is chosen for verification of the MSM due to its ability to resolve various field parameters (such as surface charge distribution, force and torque), parameter sweep capabilities, computationally efficient mesh refinement, and relative ease of use. Note that the MSM setup could be performed using any electrostatic field solver to provide the three-dimensional force field input into the MSM optimization routine.

For this scenario a cylinder measuring 3 m in length by 1 m in diameter will be modeled because it represents a simple shape with significant 3D variation from a sphere, sized similar to the once popular GEO dual-spinner configurations. This cylinder and an external sphere with a 1 m diameter are created as solid 3D shapes in Maxwell, as shown in the left hand of Fig. 2a. Perfectly conducting material properties are assigned to both shapes, and a voltage excitation of +30 kV is prescribed on both. An external surface is held at zero voltage, and is removed from system origin in each direction at 5000 times the system dimension. Next, the FEM software creates solutions for the electrostatic force and torque on the cylinder (or a more complex geometry), refining the mesh grid according to its algorithms, while the location of the external sphere is swept through the locations shown in Fig. 2b, which represent possible relative separation positions encountered in close-proximity spacecraft formations or docking scenarios. Due to the symmetry of this particular shape, analysis is necessary in only one quadrant of a plane that contains the cylinder's axis. This force and torque data set is exported to be used for a nonlinear fit to search for the optimal sphere parameters. When the modeled shape and the external cylinder intersect, Maxwell returns an empty data point, which in turn is ignored by the nonlinear fit.

Caution must be taken when comparing the force data retrieved from Maxwell to a lower order model at certain relative positions. Remember that the Multi-Sphere Method is based upon the position-dependent capacitance charge model as outlined in the previous section. This model does not capture the induced charge effects that result when the separation distance of two charged objects is very small, i.e. when the relation $r_{ij} \gg R_i$ is not true. If this is the case, the repulsion or attraction causes the charge in each conductor to be shifted away from or towards the other object. As a result, the center of charge is not at the center of the object, which can change the magnitude of the forces and torques significantly. If the MSM is populated throughout its volume with many spheres, these induced charge effects may be captured. For the scope of this paper, however, the cylinder is populated with no more than three spheres, so the induced charge effects will not be captured in the radial dimension of the cylinder. Therefore, it is necessary to ignore the data points from Maxwell with separation distances that are small enough to contain induced charge effects. Secondly, when large separation distances are considered, the solution from Maxwell can be shown to contain numerical errors. To ensure that these anomalies do not affect the MSM solution, data points with large separation distances must also be removed.

In order to determine the upper and lower bounds of the separation distances that can be used for MSM verification, a simulation is run in Maxwell with two identical spheres, over the range of separation distances chosen above. Meanwhile, the force can also be calculated using the position-dependent capacitance model for two spheres, as laid out in Eqs. (1)–(5). This Capacitive Force Model is compared to the Maxwell Force Data in Fig. 3. Both spheres have a diameter of 1 m; one sphere is held at $V_1 = +30$ kV while the other is allowed to vary through the voltages shown in the figure. In order to highlight the computational errors at large separation distances, the forces are plotted on a logarithmic scale. In this regime,

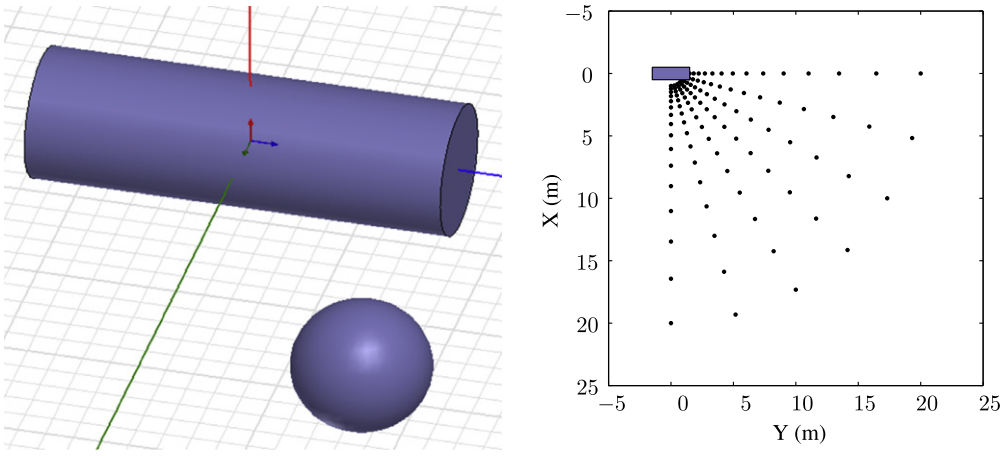

(a) Maxwell 3D model (b) Maxwell parameter sweep

Fig. 2. Maxwell 3D model and parameter sweep for data export.

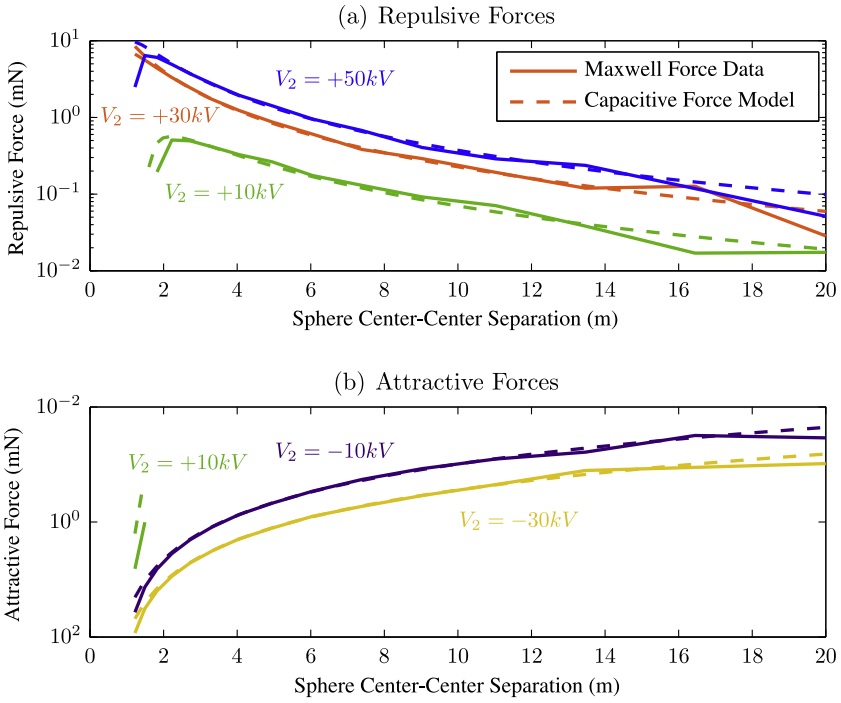

Fig. 3. Comparison between Maxwell force data and position-dependent capacitance model forces.

Maxwell looses accuracy because of the nature of FEM, which has to fill the entire volume with elements.

In this regime, the capacitive force model has been shown to match higher fidelity force evaluations using the iterative method of images solution (Seubert and Schaub, 2010). It is therefore assumed to be more accurate than the Maxwell data at these distances. At the small separation regime, the Maxwell data is known to capture the induced effects while the three-sphere model does not, and therefore these data points shall be ignored when fitting parameters to the MSM because it is not expected to capture those effects. Notice that the discrepancy in induced effects is least when both sphere have equal charge $V = +30$ kV. Outside a separation distance of 2 m, the two models agree to within 12%, suggesting the induced effects are minimal compared to the model accuracy. Within a separation distance of 15 m, the models agree to within 20%, suggesting the errors from Maxwell are on the order of the model accuracy. When verifying the model with scaled voltage values, Fig. 3 will be referenced to choose an appropriate range of separation distances.

3. Parameter selection algorithm

For the MSM to be used effectively in a six degree of freedom simulation, a set of sphere parameters needs to be selected that best reproduces the forces and torques on a given conductor shape over a full range of separation distances and orientations. An initial guess of the position and size of the spheres is chosen to model the geometry; this guess fixes the total number of spheres to be used. A nonlinear fitting scheme then compares the resulting forces and torques from the MSM to those of a trusted higher order solution (such as the FEM solver discussed above) and iterates on the parameter values until they converge to a model that optimally matches the trusted values.

3.1. Symmetry arguments

If n spheres are chosen to model a given spacecraft shape, the parameter selection algorithm needs to determine $4n$ parameters (3 spatial coordinates and a radius for each sphere). If *a priori* knowledge of the modeled shape symmetry is considered, the number of unknown parameters can be reduced, which will significantly enhance the computational time of the parameter fit. Efficiency of the nonlinear fit is not crucial as it needs to be executed only once for a given spacecraft shape preceding the model's use in simulations, but has aided considerably in the process of tuning the nonlinear fit.

For our purposes, all symmetry scenarios can be categorized as **axial** or **planar** symmetry. If the modeled spacecraft shape exhibits symmetry about a given axis, then any spheres that lie on this axis in the initial guess will remain there, thus eliminating the need to solve for off-axis coordinates. Any other spheres will be symmetrically rotated a predetermined number of times around the axis to produce p spheres. Planar symmetry is dealt with in a similar way – spheres lying on the plane will remain there, while off-planar spheres are mirrored across the plane. For the scenario in Fig. 4, with axial and planar symmetries evident in the cylinder and p chosen to be 3, only two spheres need to be specified in the initial parameter guess, but seven

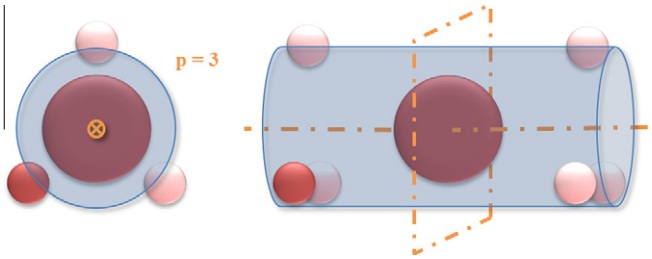

Fig. 4. Axial and planar symmetry considerations.

spheres result in the final model. Moreover, the parameter space is reduced from 28 to just 4.

3.2. Nonlinear fit

If there is a linear relationship between the parameters of a system and the output of that system, a linear regression can be performed to find an optimal solution for those parameters that minimizes some error norm between the model output and a truth output. This is even possible if the system can be linearized, but in the case of the MSM, the capacitance matrix inversion prohibits a linearization of the system. The input in this case is the external sphere position, the outputs are the force and torque values on the modeled body for that external sphere position, and the parameters are the sphere positions and sizes, as simplified by the symmetry arguments discussed above. A Gaussian least squares differential correction method is used to determine the optimal parameter set for the MSM (Junkins, 1978). Normally, this method requires partial derivatives of the model output function with respect to the parameters. The matrix inversion in the MSM model also prevents an analytical form of these partials, so a finite difference method is used.

This entire Gaussian least squares differential correction algorithm is performed by the nonlinear fit function 'nlinfit' in MATLAB. This function iteratively refits a weighted nonlinear regression, where the weights at each iteration are based on each observation's residual from the previous iteration. These weights serve to down-weight points that are outliers so that their influence on the fit is decreased. Iterations continue until the weights converge. Bisquare weights are used, which seek to find a curve that fits the bulk of the data using the usual least-squares approach, while minimizing the effect of outliers (DuMouchel and O'Brien, 1989; Holland and Welsch, 1977). Moreover, the relative weight of each data point can be prescribed which is useful if fitting to the correct forces is more important than obtaining accurate torques, for example. As with any nonlinear fit, global convergence of the optimal solution is dependent on the initial guess of the sphere parameters. A manual search is used to determine an appropriate set of initial parameters. Although the symmetry arguments as implemented above aid in the computation effort, this approach can break down when the model consists of many spheres. Other schemes to populate a given geometry with numerous spheres are being investigated. However, as shown with the results below, this MSM approach is yielding practical and implementable solutions.

4. Model verification

The algorithms described above are run to determine the optimal MSM parameters to model the electrostatic interactions of the aforementioned 1 m diameter by 3 m length cylinder. An initial guess with three spheres is chosen, where the center sphere lies at the origin and the mirrored side spheres lie along the y-axis. Remember that not the entire range of locations shown in Fig. 2b is used in the fit, but only the separation distances deemed accurate based on assessment of Fig. 3. That is, those with a surface-to-surface separation greater than 1 m and with a center-to-center separation smaller than 15 m.

The geometry of the resulting spheres, superimposed on the actual cylinder, is shown in Fig. 5, with parameters listed in Table 1. This model will be used throughout the remainder of the paper. While the spheres intersect each other in physical space, this does not present a problem in the framework of the MSM.

4.1. Quantifying fit

A large effort in the current research is in verifying the quality of the aforementioned nonlinear fit. Once a set of parameters is chosen, the accuracy of the model compared to numerical results from Maxwell must be determined. While the nonlinear fit returns a mean squared error norm that can be used to compare the quality of one fit to another, it is desirable to analyze in more detail where in the physical space surrounding the geometry a particular MSM parameter solution fits the Maxwell data well or poorly.

Figs. 6 and 7 show the visual metric that is used to analyze the quality of a given parameter set, for forces and torques respectively. In Fig. 6a, the output values from the MSM are plotted against the numerical truth model (Maxwell) at each external sphere position, with a line of slope equal to 1 to show the desired position of data points. Data points within the region used for parameter selection are shown in black, while extraneous points are shown in red.[1] While this plot shows that the current MSM over-predicts the higher forces, it does not contain any information about where these over-predictions occur, although we can gather that this happens when the external sphere is closer to the cylindrical body. Fig. 6b displays the interpolated absolute error at a given external sphere position on the x- and y-axis, using a logarithmic color scale. Because the model does not capture induced effects, which causes a de-

[1] For interpretation of color in Fig. 6, the reader is referred to the web version of this article.

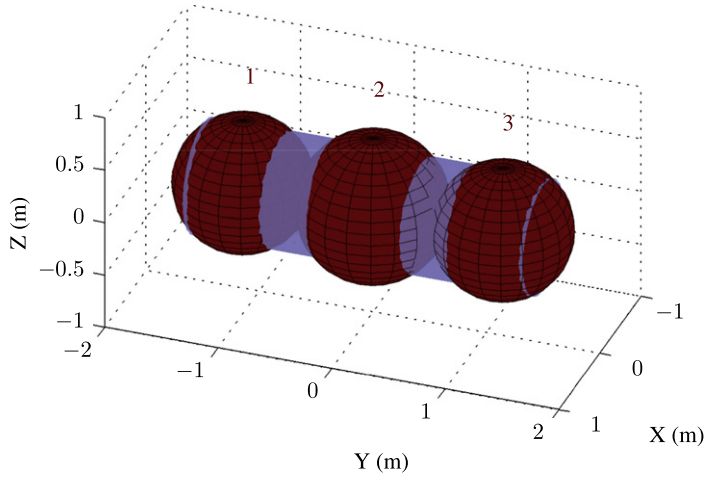

Fig. 5. Multi-Sphere Method parameters for cylinder geometry.

Table 1
Parameters of three-sphere MSM for cylinder.

	Sphere 1	Sphere 2	Sphere 3
X Coordinate (m)	0	0	0
Y Coordinate (m)	−1.1454	0	1.1454
Z Coordinate (m)	0	0	0
Radius (m)	0.5959	0.6534	0.5959

crease in the repulsion between very close like-charged objects, it over-predicts the magnitude of forces at very close separation distances. Similarly, the torques at locations shown in red are not accurately captured by the model. Therefore only the more accurate data points in the middle of the range from Maxwell are used for the MSM parameter fit.

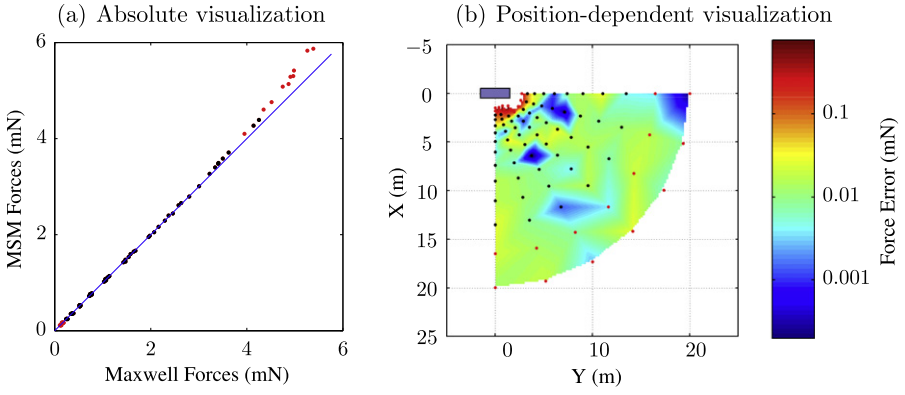

Fig. 6. Force comparison – MSM and Maxwell.

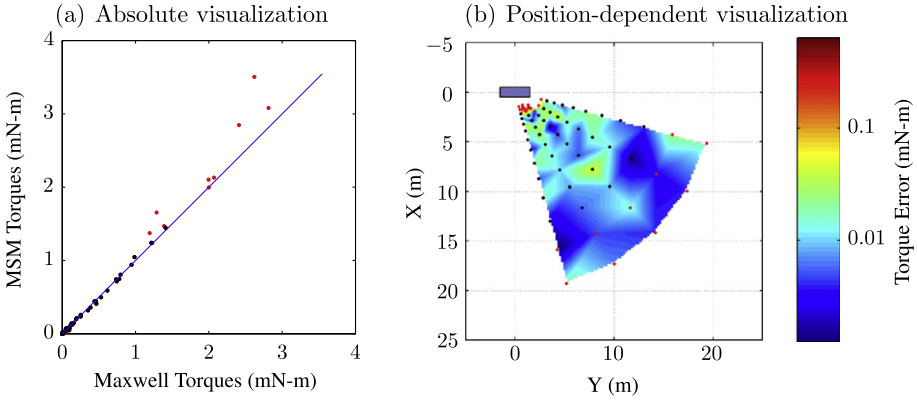

Fig. 7. Torque comparison – MSM and Maxwell.

While the visual approach to quantifying the Multi-Sphere Method above is useful for analyzing the quality of a single parameter fit, when multiple scenarios are compared to each other, it is desirable to have a single value for the quality of the fit for each scenario. The following scalar residual sums RES_F and RES_L for the model forces and torques are therefore defined. Here n is the number of external sphere locations $\boldsymbol{d}_i$ where data points are considered, and F and L refer to the forces and torques from the MSM and the Maxwell truth data.

$$RES_F = \frac{\sum_{i=1}^{n} |F_{\text{MSM}}(\boldsymbol{d}_i) - F_{\text{truth}}(\boldsymbol{d}_i)|}{\sum_{i=1}^{n} F_{\text{truth}}(\boldsymbol{d}_i)} \tag{6}$$

$$RES_L = \frac{\sum_{i=1}^{n} |L_{\text{MSM}}(\boldsymbol{d}_i) - L_{\text{truth}}(\boldsymbol{d}_i)|}{\sum_{i=1}^{n} L_{\text{truth}}(\boldsymbol{d}_i)} \tag{7}$$

Dividing by the denominator ensures that this scalar residual sum is independent of the resolution of the data set. Table 2 compares the residuals of the three-sphere MSM fit shown above and a single sphere model (equivalent to the Effective Sphere Method in Jasper and Schaub, 2011). The single sphere size is determined using the same non-linear fit, resulting in $R = 0.9974$ m. It is clear that the single sphere results in much higher residuals than the three-sphere model, and RES_L for a single sphere is unity because it lacks the ability to predict any non-zero torques.

4.2. Model scaling

An important step to validating the Multi-Sphere Method is to verify whether a model with specific parameters scales with some of the arbitrary constants that were chosen when using Maxwell to develop a truth model data set. While the geometry of the modeled shape is specified in the problem statement, the size of the external sphere R_B and the model and external sphere voltage V_A and V_B, were chosen arbitrarily, though they represent typical spacecraft charge control parameters. When the MSM is utilized in simulations, these conditions are liable to change. Moreover, the external sphere could take on a generic 3D shape of its own, which can in turn be modeled with the MSM. To verify that the specific model holds when these parameters are changed, the outputs of the MSM with the optimized sphere parameters are compared to numerical simulations while individually varying the parameters R_B, V_A and V_B and replacing the external sphere with a duplicate of the 3D body at two orientations. Remember that the nominal values are an external sphere with $R_B = 0.5$ m, $V_A = V_B = 30$ kV, and the same three-sphere model outlined in Table 1. The results are concisely summarized using scalar residual values in Table 3.

Table 2
Scalar residual comparison between three-sphere MSM and single sphere model.

	3 sphere MSM	Single sphere model
RES_F	0.0155	0.0972
RES_L	0.0485	1.0000

The residual values for all the scaled scenarios are an improvement over the single sphere residuals in Table 2. The only scenario that yields less than desirable results are the combination of $V = +30$ kV and $V = +10$ kV. Fig. 3 shows that the induced charge effects are largest for this combination of charges, which are not captured by a three-sphere MSM. Future models with multiple spheres may capture these effects better. For now, it is still clear that the three-sphere model provides an improvement over other models because of its ability to resolve torques and forces more accurately than a single sphere approximation.

5. Charge distribution in MSM

The claim was made earlier that the Multi-Sphere Method captures induced charge effects that are not included in the analytic 2-sphere solution with position-dependent capacitance considerations, but only in a dimension with multiple spheres. To verify this claim, a comparison is shown in Fig. 8 between the charge distribution on the objects in Maxwell for an external sphere in line with the cylinder, compared with the three-sphere MSM in the same orientation. To maximize the induced effects, the cylinder is given a voltage $V_A = 10$ kV while the external sphere has $V_B = 30$ kV prescribed. Clearly, the distribution of charge in the three spheres that compose the MSM matches the charge distribution in the fully resolved geometry shown in Maxwell. Where a single sphere model would place all the charge at the center of the body, the MSM has extra freedom in where the charges are distributed along the y-axis, thus capturing some of the induced charge effects.

6. Cylinder de-spin simulation

In order to demonstrate the practicality of the Multi-Sphere Method, a simulation is performed whereby a

Table 3
Scalar residual comparison of scaled parameter variation from numerical simulation.

R_B variation	0.25 m	1 m	
RES_F	0.0150	0.0578	
RES_L	0.0639	0.0749	
V_A variation	−30 kV	10 kV	50 kV
RES_F	0.0281	0.0225	0.0242
RES_L	0.0370	0.1021	0.0745
V_B variation	−30 kV	10 kV	50 kV
RES_F	0.0275	0.0733	0.0241
RES_L	0.0424	0.2454	0.0481
External cylinder	Parallel	Perpendicular	
RES_F	0.0355	0.0305	
RES_L	0.0350	0.0744	

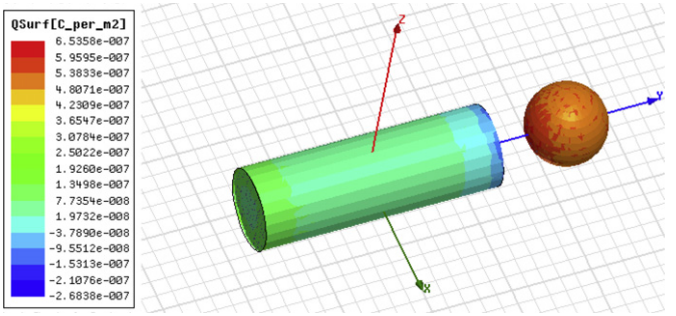

(a) Surface charge from Maxwell 3D

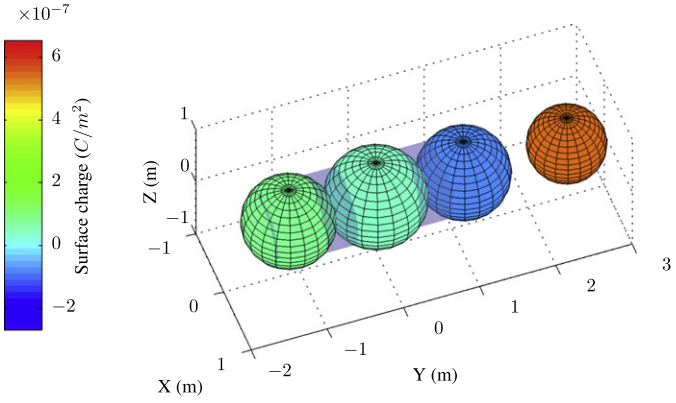

(b) Surface charge from three-sphere MSM

Fig. 8. Surface charge density comparison between Maxwell 3D and a three-sphere MSM.

sphere is used to remove the angular rotation on a cylinder using only charge control. Since this scenario requires real-time knowledge of electrostatic torques, the MSM is an elegant non-FEM model that can achieve this simulation and performs it many orders of magnitude faster. A uniform density 3 m × 1 m cylinder (as before) is placed in deep space at a constant separation distance $d = 10$ m from a sphere of radius $R = 0.5$ m, with orientation defined as in Fig. 9. This scenario represents a spacecraft (the sphere) that flies in proximity of a debris object (the cylinder). Using charge control devices such as electron or ion guns aimed at the debris cylinder or deep space, the sphere spacecraft can control both voltages V_1 and V_2 in order to de-spin the cylinder (King et al., 2002). The simulation assumes that a separate relative motion feedback control maintains a constant relative separation. This allows the study to focus on the impact of the electrostatic torques.

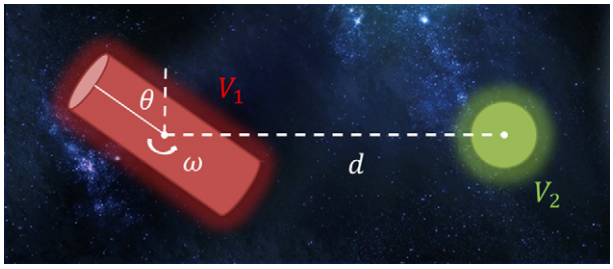

Fig. 9. Depiction of cylinder de-spin simulation.

The cylinder is constrained to rotate about its center, in the plane that it makes with the sphere, and given an initial angular velocity $\omega_0 = 2$ deg/s. A three-sphere MSM with the parameters determined earlier is used to determine the Coulomb interactions during the simulation. Further simulation parameters are given in Table 4.

While it is possible to control the final attitude of the cylinder using both equal and opposite polarities on the crafts, the scope of the de-spin simulation for this paper is limited to a rate based attitude control to remove the angular motion from the cylinder. To this end, the simplest control to implement with a charge control device is one where $V_1 = -V_2$, i.e. the sphere spacecraft transfers all its charge to the cylinder, resulting in attractive interaction. Note that there are issues with sensing and controlling the voltage on a remote body that are not addressed here. Since either polarity results in the same torques, the control is simplified further such that $0 < V_2 < V_{max}$. The rate of voltage control is not limited since charge control devices operate at a time scale that is orders of magnitude faster than the duration of this simulation. The one dimensional attitude dynamics for body 1 are

$$I\dot{\omega} = L \tag{8}$$

where L is the electrostatic torque exerted on the cylinder. The following positive semi-definite Lyapunov function is chosen,

$$V(\omega) = \frac{1}{2} I\omega^2 \tag{9}$$

with derivative

$$\dot{V}(\omega) = \omega(I\dot{\omega}) \tag{10}$$

$$= \omega L \tag{11}$$

Although the exact electrostatic torque L is not analytically known, it is possible to prove stability using only the sign of L. To start, the symmetry of the cylinder is invoked to limit its rotation parameter to $-90^\circ < \theta < 90^\circ$. When opposite polarity (i.e., attractive) control is applied between the bodies, the side of the cylinder closer to the sphere receives a stronger attraction than the far side. In other words,

$$L \begin{cases} > 0 & \text{if } \theta > 0 \\ < 0 & \text{if } \theta < 0 \end{cases} \tag{12}$$

This means that there is desirable controllability in only two of the four quadrants for any given rotation direction. Assuming a bang–bang control that turns the voltage levels either fully on or off, the following control algorithm is chosen:

		ω	
		+	−
θ	+	OFF	ON
	−	ON	OFF

Table 4
Parameters for cylinder de-spin simulation.

Parameter	Value	Units	Description
d	10	m	Object center-to-center separation
ρ	100	kg/m^2	Object densities
m_1	235.6	kg	Cylinder mass
I_1	191.4	kg m^2	Cylinder transverse moment of inertia
ω_0	2	deg/s	Initial cylinder angular velocity
V_max	30	kV	Maximum control voltage

This control law can also be expressed as follows, where $H()$ represents the Heaviside function:

$$V_1 = -V_{max}H(-\theta\omega)$$
$$V_2 = +V_{max}H(-\theta\omega) \quad (13)$$

Since $L = 0$ when the control is off, and $\text{sign}(L) = \text{sign}(\theta)$ when the control is on as in Eq. (12), inspection shows that the Lyapunov rate in Eq. (10) is negative semi-definite, i.e.

$$\dot{V}(\omega) \leqslant 0 \quad (14)$$

Therefore, the rate of the cylinder is guaranteed to be driven to zero.

Using the control law above, it takes roughly 64 h for the cylinder to stop rotating, as shown in Fig. 10. More often than not, due to discrete time steps of the simulation, the cylinder will be stopped at $\theta = \pm 90^\circ$. Faster de-spin, as well as cylinder attitude control could be achieved if the spherical craft contained a secondary charge control device, which would allow for same polarity charging of the two craft. A 2 deg/s initial rotation is not especially large, but considering the time scale of most space maneuvers, this is a very promising result for the de-spin of a debris object. Such actions might be required for missions that attempt to attach to debris objects in order to de-orbit them. The MSM is notably quick in resolving the torques required for this simulation. The entire de-spin simulation is completed in several minutes on a desktop computer, while it takes Maxwell 3D more than a minute to resolve the forces and torques for a single orientation.

From Fig. 7, the three-sphere MSM is shown to approximate the torques to within 30% of the truth value from Maxwell for a 10 m separation distance. This discrepancy is to be expected since the nominal torques at this separation distance are very small, and computational errors are present in Maxwell. To analyze the effects of torque uncertainties, the simulation was re-run using a 30% increase and decrease in the torque value used to resolve the dynamics. When the MSM in the controller under-predicted the torque value, it takes 18% less time for the debris object to stop making full rotations, but removing the remaining oscillations is slower. If the MSM over-predicts the actual torque values, the debris takes 31% longer to despin, but the asymptotic convergence to zero motion occurs in roughly the same amount of time. These are the extremes for model uncertainty.

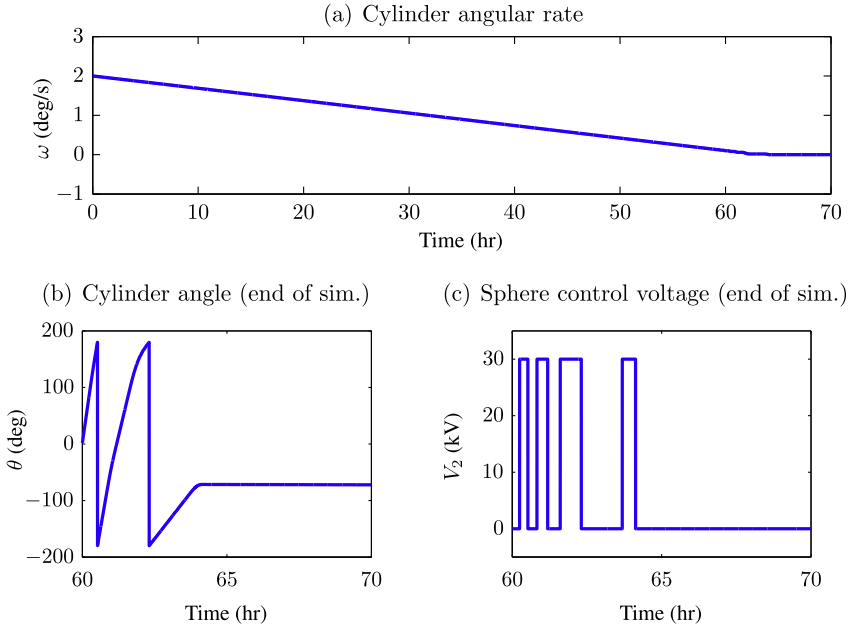

Fig. 10. Cylinder de-spin simulation using voltage control on proximity sphere.

7. Conclusion

This paper introduces the Multi-Sphere Method (MSM), a reduced order, computationally efficient electrostatic model that captures the three dimensional Coulomb effects of generic conducting shapes. This version of the MSM assumes the body has a fully conducting outer surface which is held at a common absolute potential. A methodology is presented to create approximate three-dimensional electric force fields using a small number of optimally placed spheres. It is found that even with a small number of spheres to approximate a cylinder, the nonlinear sphere parameter optimization can become challenging. While symmetry arguments are included to decrease the computational intensity of the nonlinear fit, an open question remains on how well this MSM method will scale to large number of internal spheres. While the presented MSM cylinder solution can capture net forces and torque acting on a body if the separation distances are larger than 1 body length, a future challenge is to refine this method to model the up-close electric fields right up to the point of contact. The 3-sphere MSM model is a convenient solution as many GEO debris objects such as rocket bodies and dual-spinners have this shape. The presented work will enable future relative dynamics and control studies where the full 6 degrees of freedom motion can be rapidly simulated. Further, these presented solutions are also applicable for control optimizations algorithms that require very rapid force evaluations. Future work will investigate simplifications to the MSM setup procedure which scale more readily to larger numbers of spheres.

Acknowledgments

This material is based upon work supported by the NASA Science & Technology Research Fellowship (NASA Grant #NNX11AN47H).

References

Berryman, J., Schaub, H. Analytical charge analysis for 2- and 3-craft coulomb formations. AIAA Journal of Guidance Control and Dynamics 30 (6), 1701–1710, 2007.

Denton, M.H., Thomsen, M.F., Korth, H., Lynch, S., Zhang, J.C., Liemohn, M.W. Bulk plasma properties at geosynchronous orbit. Journal of Geophysical Research A7, 110, 2005.

DuMouchel, W.H., O'Brien, F.L. Integrating a robust option into a multiple regression computing environment, in: Computer Science and Statistics: Proceedings of the 21st Symposium on the Interface. American Statistical Association, Alexandria, VA (Manuscript), 1989.

Hogan, E., Schaub, H. Relative motion control for two-spacecraft electrostatic orbit corrections. in: AAS/AIAA Spaceflight Mechanics Meeting, Girdwood Alaska. Paper AAS 11-466, 2011.

Hogan, E., Schaub, H. Collinear invariant shapes for three-craft coulomb formations. Acta Astronautica, 12:78–89, 2012.

Holland, P., Welsch, R. Robust regression using iteratively reweighted least-squares. Communications in Statistics: Theory and Methods A6, 813–827, 1977.

Jasper, L.E.Z., Schaub, H. Effective sphere modeling for electrostatic forces on a three-dimensional spacecraft shape. In: AAS/AIAA Spaceflight Mechanics Meeting. Girdwood Alaska. Paper AAS 11-465, 2011.

Junkins, J. Optimal Estimation of Dynamical Systems, first ed. Sijthoff-Noordhoff, 1978.

King, L.B., Parker, G.G., Deshmukh, S., Chong, J.H. Spacecraft formation-flying using inter-vehicle coulomb forces. Technical Report NASA/NIAC. http://www.niac.usra.edu, 2002.

King, L.B., Parker, G.G., Deshmukh, S., Chong, J.H. Study of interspacecraft coulomb forces and implications for formation flying. AIAA Journal of Propulsion and Power 19 (3), 497–505, 2003.

Natarajan, A., Schaub, H. Linear dynamics and stability analysis of a coulomb tether formation. Journal of Guidance Control and Dynamics 29 (4), 831–839, 2006.

Parker, G.G., Passerello, C.E., Schaub, H. Static formation control using interspacecraft coulomb forces. In: 2nd International Symposium on Formation Flying Missions and Technologies. Washington D.C., 2004 (Manuscript).

Schaub, H. Stabilization of satellite motion relative to a coulomb spacecraft formation. Journal of Guidance Control and Dynamics 28 (6), 1231–1239, 2005.

Schaub, H., Jasper, L.E.Z. Circular orbit radius control using electrostatic actuation for 2-craft configurations. In: AAS/AIAA Astrodynamics Specialist Conference. Girdwood, Alaska. Paper AAS 11–498, 2011.

Schaub, H., Moorer, D.F. Geosynchronous large debris reorbiter: Challenges and prospects. In: AAS Kyle T. Alfriend Astrodynamics Symposium. Monterey, CA; . Paper No. AAS 10-311, 2010.

Schaub, H., Parker, G.G., King, L.B. Challenges and prospect of coulomb formations. Journal of the Astronautical Sciences 52 (1–2), 169–193, 2004.

Schaub, H., Hall, C., Berryman, J. Necessary conditions for circularly-restricted static coulomb formations. Journal of the Astronautical Sciences 54 (3–4), 525–541, 2006.

Seubert, C.R., Schaub, H. Closed-loop one-dimensional charged relative motion experiments simulating constrained orbital motion. In: AAS/AIAA Astrodynamics Specialist Conference. Pittsburgh, PA., 2009a (Manuscript).

Seubert, C.R., Schaub, H. One-dimensional testbed for coulomb controlled spacecraft studies. In: AAS/AIAA Spaceflight Mechanics Meeting. Savannah, Georgia; 2009b (Manuscript).

Seubert, C.R., Schaub, H., Electrostatic force model for terrestrial experiments on the coulomb testbed. In: 61st International Astronautical Congress. Prague, CZ: International Astronautical 'Federation. Paper IAC-10.C1.1.9, 2010.

Sliško, J., Brito-Orta, R.A. On approximate formulas for the electrostatic force between two conducting spheres. American Journal of Physics 66 (4), 352–355, 1998.

Smythe, W.R. Static and Dynamic Electricity, third ed. McGraw-Hill, 1968.

Soules, J.A. Precise calculation of the electrostatic force between charged spheres including induction effects. American Journal of Physics 58 (12), 1195–1199, 1990.

Tribble, A.C. The Space Environment – Implications for Spacecraft Design, revised and expanded ed Princeton University Press, 2003.

Vasavada, H., Schaub, H. Analytic solutions for equal mass four-craft static coulomb formation. Journal of the Astronautical Sciences 56 (1), 17–40, 2008.